ELSEVIER

S0032-3861(96)00063-8

Polymer Vol. 37 No. 23, pp. 5131–5137, 1996

0032-3861/96/$15.00 + 0.00

On-line measurements of orientation induced crystallization of PET during high speed spinning

H. Hirahata*, S. Seifert and H. G. Zachmann
Institut für Technische und Makromolekulare Chemie, University of Hamburg, Germany

and K. Yabuki†
Toyobo Research Institute, Kataka, Japan
(Received 3 July 1995)

An experimental set-up in the synchrotron radiation beam was constructed for performing wide angle X-ray scattering (WAXS) on-line measurements, during high speed spinning of poly(ethylene terephtalate) (PET). In order to detect the very weak scattering of the thin filaments (= 26 μm diameter) the capton windows of the vacuum tubes were removed and the air was replaced by helium. In this way it became possible to measure the development of crystal reflections as a function of the distance from the spinneret. A comparison of the results with corresponding on-line measurements of the fibre diameter indicates that crystallization starts at the beginning of the necking zone. Copyright © 1996 Elsevier Science Ltd.

(Keywords: PET; high speed spinning; orientation induced crystallization; WAXS; synchrotron radiation; neck-like deformation)

INTRODUCTION

Orientation induced crystallization during spinning of fibres is one of the most interesting subjects. From the scientific point of view it is interesting to study the relation between elongational flow, orientation, and crystallization. In industry, in order to lower the production costs, fibre spinning, under the condition that orientation and crystallization take place during the spinning, is much favoured. This involves that the spinning speed has been gradually increased in the past two decades[1] to speeds up to almost 10 000 m min^{-1}.

From measurements performed by different methods it is known that some interesting effects occur during high speed spinning. Following first investigations of Perez and Lechuse[2], Kikutani *et al.*[3] have measured the filament temperature and the diameter along the spinline in a high speed melt spinning experiment. At a take-up velocity of 6000 m min^{-1} a neck-like deformation was observed at a distance of 140–150 cm from the spinneret. The temperature profile showed a maximum just after the end of this deformation. The temperature at the maximum was about 160°C and the birefringence was 0.108. This maximum of the temperature was interpreted to be due to crystallization as a consequence of the orientation induced by the neck-like deformation. When sodium stearate was added as a nucleating agent the diameter profile remained the same while the position of the neck-like deformation appeared at a slightly smaller distance from the spinneret and stress and orientation just after the neck-like deformation were a little larger[4]. A neck-like deformation was also observed with poly(butylene terephthalate)[5], poly(phenylene sulfide)[6] and even in low speed spinning of polyethylene[7]. Furthermore, it was shown that the position of the neck fluctuates within a range of several centimetres[5].

More information on the development of structure and molecular orientation during spinning can be obtained by means of on-line X-ray scattering measurements during spinning. Such wide angle X-ray scattering (WAXS) studies have been already performed on various rapidly crystallizing polymers using conventional X-ray methods[8–16]. In these polymers crystallization occurred at moderate spinning speeds. It is much more difficult to perform such measurements during high speed spinning. This is due to the fact that in this case a very small filament diameter (approx. 20 μm) has to be used in order to obtain a crystalline fibre. Under these conditions the X-ray scattering becomes very weak and difficult to detect. The only investigation known is that of Haberkorn *et al.*[17] on polyamide 6 and polyamide 6.6 at take-up velocities up to 5300 m min^{-1}. They observed necking and the onset of crystallization somewhere within or at the end of the necking zone. A more exact location of the onset of crystallization in relation to the necking zone was not possible because of the fluctuation of this zone. To measure the X-ray scattering they had to use exposure times of 2–3 h.

Synchrotron radiation as a strong source for X-rays made it possible to perform measurements of the WAXS and of the small angle X-ray scattering (SAXS) within less than 1 min[18,19]. Therefore it seems appropriate to undertake further investigations of the crystallization process during spinning by using this strong radiation

* On leave of absence from TOYOBO Research Institute
† To whom correspondence should be addressed

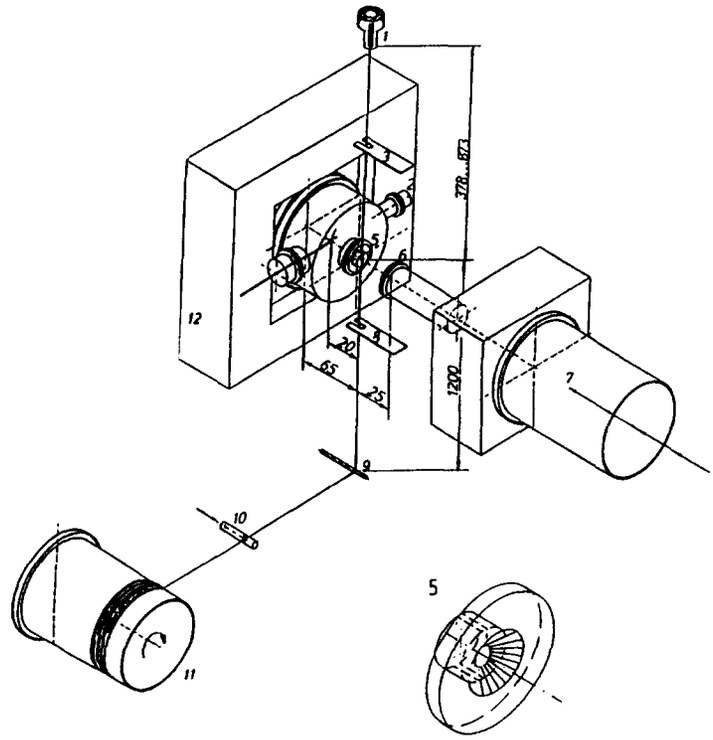

Figure 1 Experimental set-up for WAXS on-line measurement during high speed spinning of poly(ethylene terephtalate) (PET): 1, spinneret with four orifices; 2, helium; 3, ceramic guide; 4, beamstop; 5, brass guide; 6, capton window; 7, synchrotron beam; 8–10, ceramic guide; 11, godet roll; 12, 2D Gabriel detector

source. Such measurements have been performed by us on polypropylene[20] and poly(vinylidenefluoride)[20,21] using take-up velocities up to 200 m min^{-1}. In addition to the WAXS, the SAXS was detected and it was shown that a peak in SAXS was obtained before crystal reflections in the WAXS pattern became visible.

We have now improved the spinning equipment so that we can use take-up velocities up to 4300 m min^{-1} and thus perform high speed spinning experiments. In the present work we want to describe an experimental set-up for these experiments and report some results obtained with poly(ethylene terephthalate) (PET).

EXPERIMENTAL

Material

PET from Toyobo Co. Ltd., showing an intrinsic viscosity of 1.0 dl g^{-1} in *p*-chlorophenol/tetrachloroethane (60/40 by volume) at 30°C was used for extrusion. The material was dried in vacuum at 120°C for 16 h before it was filled into the extruder.

Extruder

A single screw extruder from the company Brabender with a screw diameter of 20 mm was used in connection to a metering pump. The polymer was extruded through a spinneret with four orifices each having a diameter of 0.5 mm and a length of 2 mm. The total extrusion rate was 10 g min^{-1}, i.e. 2.5 g min^{-1} per orifice. The temperature of the spinneret head and the orifice was 308°C. The temperature of the screw was 245°C (zone 1) and 295°C (zone 2). The spin block and the metering pump had a temperature of 305°C. The intrinsic viscosity after extrusion was 0.8 dl g^{-1}.

The extruded fibre was wound up on a godet roll (11 in *Figure 1*) with a diameter of 190 mm after passing through two ceramic guides (9 and 10 in *Figure 1*), the last one placed just before the godet roll. The rotation frequency of the godet roll could be continuously varied between 14 and 120 Hz resulting in take-up velocities between 500 and 4300 m min^{-1}.

WAXS measurements

The WAXS measurements were performed at the Hamburg Synchrotron Radiation Laboratory (HASYLAB) at DESY in Hamburg using the double focusing camera of the polymer beamline[18,19]. The synchrotron radiation was monochromatized by Bragg reflection on a germanium single crystal. The primary beam intensity was measured by an ionization chamber and the scattering intensity was normalized by dividing it by the intensity of the primary beam. Further details of the beamline can be found elsewhere[18,19].

The extruder was mounted on a platform which could be moved vertically with help of a stepper motor drive system (see *Figure 1*). Since the position of the synchrotron beam is fixed, the distance between the measuring point and the spinneret was varied by moving the extruder up and down. In this way the distance between the spinneret and the synchrotron beam could be varied between 38 and 87 cm. The filaments were kept within the synchrotron beam by means of two ceramic guides (3 and 8 in *Figure 1*) just above and below the synchrotron beam.

The greatest difficulties in performing the WAXS measurements arose from the small diameter of the filaments which, at the position where crystallization occurred, was about 26 μm only. With the usual experiment set-up consisting of a vacuum tube in front and one behind the fibre and air surrounding the fibre in the gap between the two tubes, the scattering of the windows (thin films of capton) together with that of the

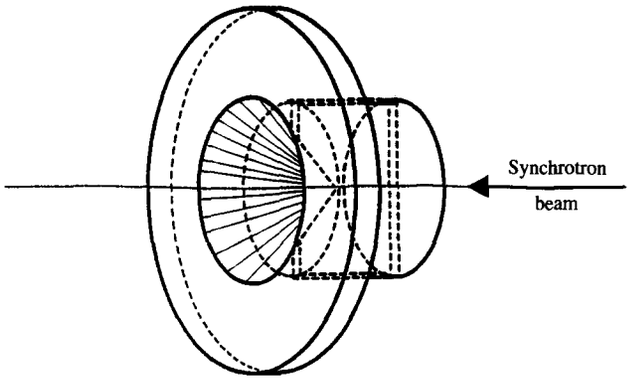

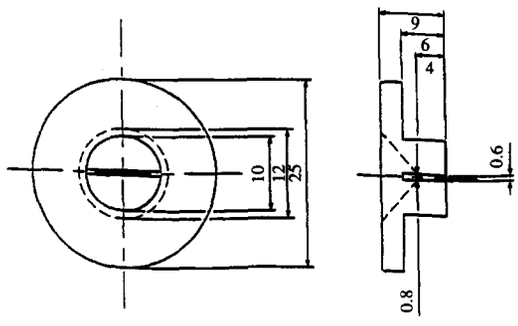

Figure 2 Aperture shown in *Figure 1* guide-5

air was so strong that it was not possible to separate it from that of the fibre. As the situation could not be improved by using other materials as windows namely Mylar, beryllium or a mica sheet, we finally removed the windows from the tube between the fibre and the detector (left side of the fibre in *Figure 1*) and filled this tube by helium. The helium was allowed to flow through the window 5 and thus replace the air in front of the fibre. The flow rate was approx. 4 l min^{-1}.

Furthermore, a specially designed metal aperture (5 in *Figure 1*) with a slit having a length of 10 mm and a width of 0.6 mm was placed in front of the window 5 in order to diminish the background scattering in equatorial direction arising from the windows and the remaining air. This aperture is represented in more detail in *Figure 2*. Since the width of the slit was smaller than that of the synchrotron beam, a strong edge scattering of the slit was observed in meridional direction. However, due to the geometry of the aperture, no such scattering occurred in equatorial direction where the appearance of crystal reflections was expected. With help of the helium and this aperture the unwanted scattering was so much reduced that it became possible to detect the crystal reflections of the filament.

The scattered intensity was measured by means of a two-dimensional wire detector (Gabriel detector)[22,23]. The accumulation time was 2.5 min. After each measurement the background of the detector was determined by closing the aperture in front of the detector. In addition the scattering of the set-up without fibre (scattering of windows, remaining air etc.) was determined. First we have only subtracted the background of the detector from the total scattering to obtain the scattering from the

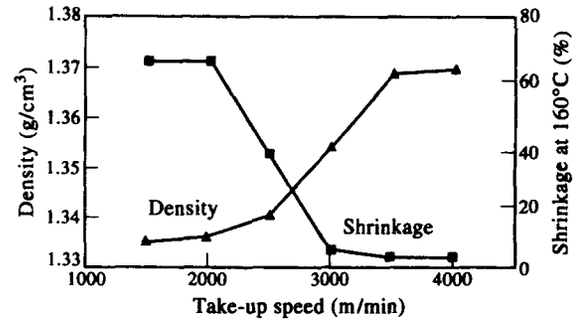

Figure 3 Density at 30°C and shrinkage at 160°C of the fibre after spinning as a function of the take-up velocity

fibres plus that of the windows and the air. Second we have also subtracted the background scattering from the experimental set-up in order to determine the scattering from the fibres alone. A comparison of the results with and without background scattering of the experimental set-up was necessary in order to get information on the reliability of the results.

Measurements of the filament diameter

On-line measurements of the diameter profile of one filament during spinning were performed by means of the Diameter Monitor 460 A/2 from the company Zimmer (Frankfurt). This monitor generates an analogue signal, which is proportional to the diameter of the fibre, by measuring the fraction of light reflected by the fibre. The instrument had to be calibrated by means of a fibre with known diameter.

Density measurements

The densities of the fibres were measured in a density gradient tube containing a mixture of hexane/tetrachloroethane.

RESULTS

In order to find the appropriate spinning conditions for the on-line experiments, we have first studied the influence of the take-up velocity on the crystallinity and orientation of the final fibre. *Figure 3* shows the density at 30°C and the shrinkage at 160°C as a function of the take-up velocity. At 2500 m min^{-1} an increase of density is observed indicating that the material has started to crystallize. As a consequence of the network formed by the crystals, the hot air shrinkage is decreased. At 3000 m min^{-1} the crystallinity is already so large that the hot air shrinkage is almost negligible. At 3500 m min^{-1} the degree of crystallinity has reached its maximum value. According to these results, we used a take-up velocity of 4000 m min^{-1} in our following diameter profile and WAXS measurements.

Figure 4 shows the diameter of a filament d at 4000 m min^{-1} as a function of the distance from the spinneret h. A necking deformation was clearly observed between $h = 39.8$ and 47.3 cm. At the beginning of the necking zone the diameter d is around 60 μm, at the end d is 27 μm. The position of the necking was slightly fluctuating. At $h = 42.3$ and 44.8 cm, d sometimes decreases to its minimum value (27 μm). At $h = 39.8$ cm the diameter also sometimes decreases, however never reaches the minimum value.

Figure 5 shows some two-dimensional scattering

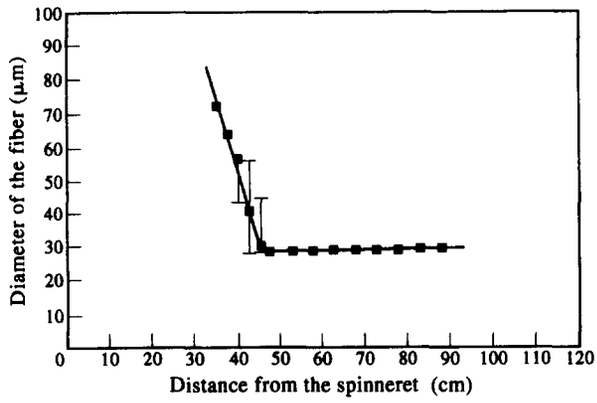

Figure 4 Diameter of the filament d as a function of the distance h from the spinneret during spinning at 4000 m min^{-1}. The necking zone is indicated by (■)

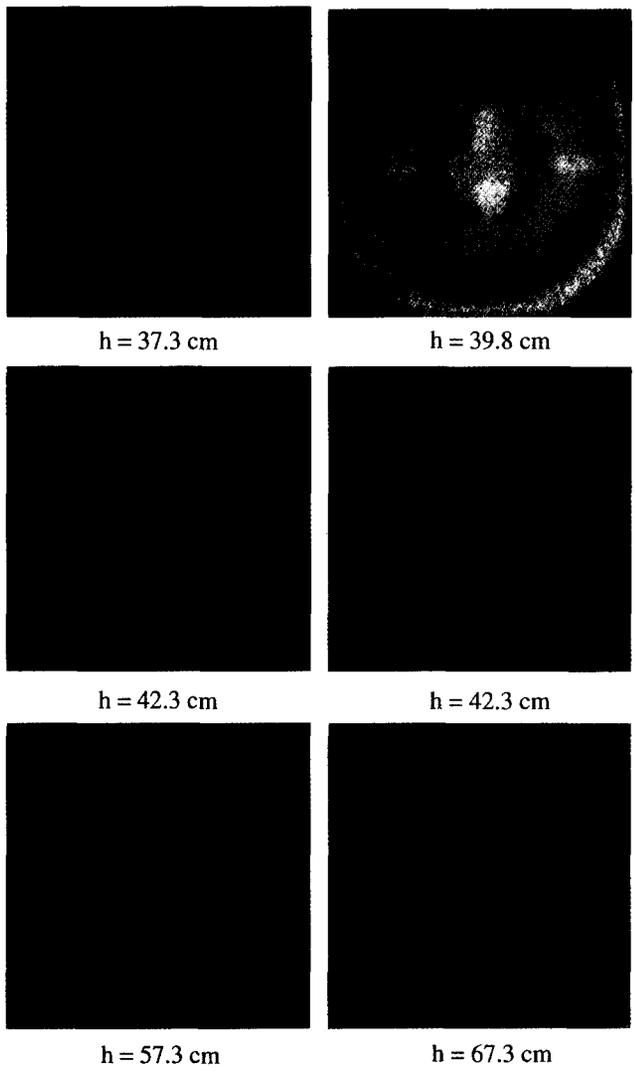

Figure 5 Two-dimensional scattering patterns at various distances h from the spinneret during spinning at 4000 m min^{-1}

patterns obtained at various distances h from the spinneret. In the two patterns at the bottom of the figure, obtained at $h = 57.3$ and 62.3 cm, one can clearly recognize the three crystal reflections (100, 110 + 111, 010 + 011) of PET on the equator. The strong scattering along the meridian is an artifact. It arises from the air and the metal edges (see Experimental part). Patterns showing strong crystal reflections were always obtained

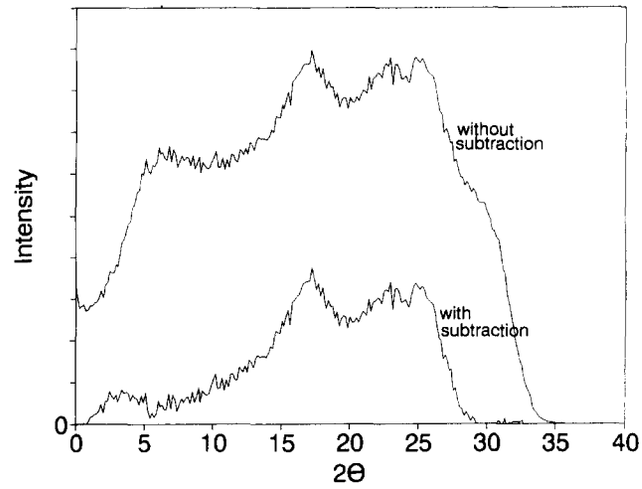

Figure 6 Scattering intensity along the equator as a function of the scattering angle 2Θ at $h = 57.3$ cm before and after subtraction of the background scattering during spinning at 4000 m min^{-1}

at distances exceeding the value $h = 49.3$ cm, i.e. after the end of the necking zone.

If h was smaller than 39 cm, no X-ray crystal reflections were observed. The scattering diagrams obtained at these values of h looked like the one shown on the upper left side of *Figure 5* measured at $h = 37.3$ cm. One can only recognize the strong background scattering on the meridian. The amorphous halo is not visible because it is too weak.

At distances of h between 39.8 and 47.3 cm, in some measurements crystal reflections were observed while in other measurements no such reflections appeared. This is illustrated by the patterns at $h = 42.3$ cm and is due to the fluctuation of the necking zone. However, it is worthwhile to note that crystal reflections were not only observed at 42.3 cm, but in some cases also at 39.8 cm (upper figure, right-hand side) where, according to our diameter measurements, necking in no case was completed.

From the small azimuthal half width of the crystal reflections it follows that the orientation of the crystals is very high from the beginning of crystallization and does not considerably increase during further crystallization. At $h = 47.3$ cm a value of 0.92 is obtained for the Herman orientation function of the 100 reflection with respect to the equator.

Figure 6 shows the scattered intensity at $h = 57.3$ cm as a function of 2Θ, where 2Θ is the scattering angle, along the equator before and after subtraction of the background scattering arising from the set-up. In order to decrease the noise for each reflection an average of the intensity over 15 channels of the detector in azimuthal direction was calculated. Though the scattering of the sample is only 20% of the background scattering one can clearly recognize the crystal reflections in both curves. The noise, however, is comparatively large. Therefore, we have smoothed the scattering curves by convolution with a Gaussian function having a half width of $\Delta(2\Theta) = 1.1°$ just removing the rapid fluctuation while leaving the crystal reflections almost unaffected. This procedure increased the half width of the crystals by 25% which does not affect the evaluation. *Figure 7* shows the smoothed intensity as a function of 2Θ at different distances from the spinneret after subtraction of the background and smoothing as described above. In agreement with *Figure 5*, crystal reflections appear when h is larger than 49 cm and also, in some cases, at

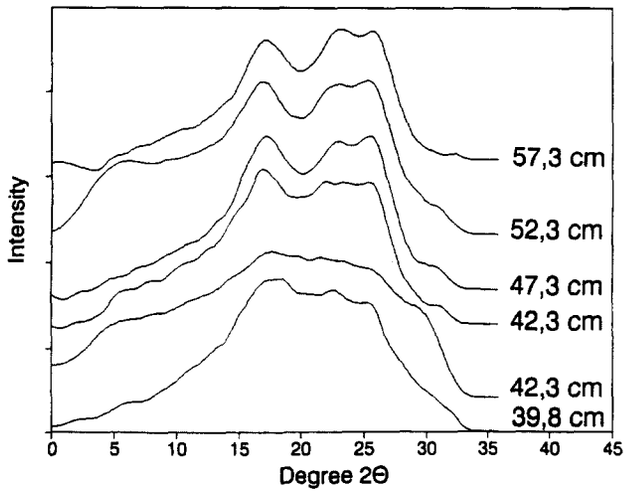

Figure 7 Smoothed scattering intensity along the equator as a function of the scattering angle 2Θ of different distances from the spinneret during spinning at 4000 m min^{-1}

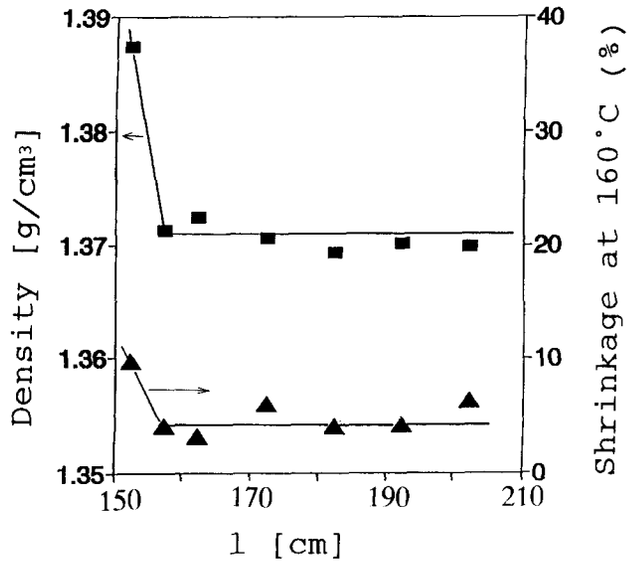

Figure 8 Density and shrinkage of the fibre after spinning at 4000 m min^{-1} as a function of the distance l between spinneret and guide 9 (see *Figure 1*)

smaller values of h however never at values below 39.8 cm. One can see an increase of the intensity of the crystal reflections with increasing distance h of the spinneret. The main increase, takes place within or slightly after the necking zone.

DISCUSSION

Influence of the guides and of the helium on the spinning process

The guides 3 and 8 in *Figure 1*, the slit in the aperture shown in *Figure 2* and, finally, the application of helium, are not used under normal spinning conditions but are necessary in our experiments in order to make the WAXS measurements possible. How do these devices influence the spinning process?

For helium, the molar heat capacity is smaller and the thermal conductivity is larger than for air. Therefore the cooling of the filaments and consequently the temperature profile along the filaments are expected to change if helium is used instead of air. However, in our set-up the helium is blown onto the fibre just at the location where the X-ray scattering is measured. As a consequence of the air drag, the helium will be drawn downwards and no helium will flow in the area above the point at which the scattering is measured. Therefore we conclude that the temperature profile, if at all, will only be changed below the region from which the scattering is measured and will not affect the diameter profile and the crystallization above and within this region.

The guides 3 and 8 in *Figure 1* and the slit in the aperture shown in *Figure 2* may change the temperature and the stress of the filaments if they come into contact with the filaments. It is very difficult to estimate the changes of the spinning conditions caused by this effect. We have measured the stress of the filament during spinning with and without these guides and have noticed no difference.

Due to special restrictions in the experimental chamber, the spin-line used in our experiments was comparatively short. The maximum distance l between the spinneret and the guide 9 in *Figure 1* was only 207.3 cm. If the temperature of the filament is not low enough when this guide is passed, some additional drawing may take place between this guide and the godet roll. In order to find out to which extent this effect is present the following experiment was performed: at a constant take-up velocity of 4000 m min^{-1} the total length of the spin-line was varied by moving the extruder up and down. The densities at 30°C and shrinkage at 160°C of the final fibres obtained at different positions of the extruder were measured. *Figure 8* represents the results as a function of the distance l between the spinneret and the guide 9. As one can seen, constant values are obtained for $l = 157.3$ cm and more. An increase in density (crystallinity) and shrinkage is found only when l is 152.0 cm. This increase is considered to be a consequence of additional drawing between the guide 9 and the godet roll. From the constant values for $l > 157.3$ cm it is concluded that no additional drawing occurs for positions of the extruder at this distance. As all measurements were performed at $h > 37.3$ cm corresponding to $l > 157.3$ cm we can exclude an additional unwanted drawing between the guide 9 and the godet roll in our measurements.

Dependence of crystallization of the fibre on the take-up velocity

Usually orientation induced crystallization is only observed when the take-up velocity exceeds the value of 5000 m min^{-1}. In our case according to *Figure 3*, crystallization already starts at 2500 m min^{-1} and reaches its maximum values at 3500 m min^{-1}. This is attributed to the comparatively high molecular weight of our material which has an intrinsic viscosity of 1.0 dl g^{-1} in *p*-chlorphenol/tetrachloroethane (60/40) corresponding to $M_W = 80\,000$ g mol^{-1} while usually the viscosity is 0.7 dl g^{-1} and M_W is 50 000 g mol^{-1}.

Our previous investigations[24–26] with amorphous PET films have shown that the birefringence obtained at temperatures between 82 and 95°C by drawing does not only depend on the temperature, the draw rate and the draw ratio but also on the molecular weight M_W of the material. Keeping all other conditions the same, the birefringence was the higher the larger M_W. It seems reasonable that this must also be true for high speed spinning which can be considered to be a drawing at

higher temperatures with much larger drawing rates. Therefore we have to conclude that the critical orientation necessary for crystallization is reached at a spinning rate which is the lower the higher the molecular weight.

In which part of the necking zone does crystallization start?

Based on measurements of the temperature and diameter profile, Kikutani *et al.*[3] have concluded that crystallization proceeds rapidly just after the end of the necking process and is induced by the orientation of the chains. The necking itself can be explained by rheological effects assuming some special dependence of viscosity on temperature. According to Haberkorn *et al.*[17] necking occurs at the point where the temperature becomes so low that, at the rate of elongation applied there, the chain entanglements act as fixed netpoints and a rubber-like strong elongation occurs accompanied by a high orientation of the chains. Crystallization, again, is considered to be a consequence of this chain orientation. It should occur at the end of the necking zone where orientation is completed.

By contrast, our results indicate that in PET, crystallization already starts just after the beginning of the necking zone. We have to admit that in our case the filament thickness and the WAXS were not measured simultaneously. However, as we have repeated our measurements several times and have never found that necking started above $h = 39.3$ cm where the appearance of crystal reflections could be observed, we believe that our conclusion is supported by our experiments. The assumption that, in PET, necking is caused by the onset of crystallization is well supported by calculations performed by Katayama and Yoon[27]. They show that necking starts at a distance from the spinneret where a plateau begins to appear in the temperature curve. The plateau is interpreted to be caused by the heat of crystallization. Furthermore, the calculated stress at the necking point agrees with the necking stress measured at a PET film which was crystallized at 120°C prior to necking.

How can crystallization start in the comparatively weakly oriented fibre at the beginning of the necking zone? We believe that the orientation is not uniform. Even when the average orientation, as measured by WAXS or birefringence, is comparatively weak, a small part of the chains, in the regions where the entanglements of the chains are more stable, will become highly oriented. These chains are acting as crystal nuclei. In addition, these nuclei may act as netpoints and lead to an increase of orientation and to necking. This effect may occur in addition to the entanglement effect discussed by Haberkorn *et al.*[17]. We want to point out that evidence for growing of highly oriented crystals in an apparently unoriented amorphous matrix has been already obtained in our investigation of melt spinning of polypropylene and poly(vinylidenefluoride)[20,21] at moderate spinning speeds.

How could one explain the result that the temperature maximum is found at the end of the necking zone while crystallization starts at the beginning of this zone? One can estimate that, at 6000 m min^{-1}, it takes, roughly, 10 ms for a volume element of the fibre to move from the beginning to the end of the necking zone. It could be that this is the time which is necessary for the heat production and transfer.

One could think that in the case of the polyamides, too, the crystallization already starts at the beginning of necking despite the results of Haberkorn *et al.* obtained by X-ray scattering. In their investigation there is no indication that the amorphous halo becomes anisotropic before or just at the beginning of crystallization. A strong orientation of the amorphous chains as obtained by drawing with necking should manifest itself by a concentration of intensity of the amorphous halo on the equator. Furthermore, even in the case of simultaneous measurements of WAXS and filament thickness in the work of Haberkorn *et al.* one has to consider that the fluctuations of the neck occur on a time scale of seconds while the time necessary to measure the WAXS was 2 h. Therefore it seems to us problematic to relate the position of the end of the necking zone to the position from which the WAXS is detected. The WAXS is always averaged over different locations within the necking zone.

Obviously it is an experimentally very difficult problem to locate exactly the position where crystallization starts with respect to the necking point. In further experiments we will try to improve the set-up so that we will be also able to detect the amorphous halo and thus the orientation of the amorphous chains. Furthermore, in the case of PET, we will try to follow crystallization at scattering angles where the −105 reflection appears. Close to this reflection highly oriented amorphous material shows a sharp peak arising from an intramolecular periodicity. This peak will be used for the detection of the orientation of the amorphous chains.

CONCLUSION

By using synchrotron radiation it is possible to measure the WAXS of thin filaments (26 μm) of PET during high speed spinning within minutes. Such on-line measurements in combination with measurements of the filament thickness prove that the main part of the crystallization process takes place within the necking zone. There is some indication that crystallization starts at the beginning of necking and that crystal nuclei acting as net-points in the amorphous phase are responsible for the strong orientation by necking.

ACKNOWLEDGEMENT

This work was partly funded by the German Federal Ministry of Science on Technology (BMFT) under the contract number 05-5 GUHXB.

REFERENCES

1 Ziabicki, A. and Kawai, H. 'High-Speed Fiber Spinning', Wiley, 1985
2 Perez, G. and Lecluse, C., Proc. 18th Int. Man-Made Fibre Conf., Dornbirn, Austria, 20–22 June, 1979
3 Kikutani, T., Kawahara, Y., Matsui, T., Takaku, A. and Shimizu, J. *Seikei-kako* 1989, **1**, 333
4 Kikutani, T., Yamada, H., Takuku, A. and Shimizu, J. *Sen-i Gakkaishi* 1988, **44**, 317
5 Kikutani, T., Matsui, T., Takaku, A. and Shimizu, J. *Sen-i Gakkaishi* 1989, **45**, 441
6 Kikutani, T., Wakayama, K., Sato, M. and Takaku, A. *Sen-i Gakkaishi* 1998, **48**, 549
7 Ishizuka, O. and Koyama, K., Ref. 1, p. 151
8 White, J. L. and Cakmak, M. *Adv. Polym. Techn.* 1986, **6**, 295

9 Spruiell, J. E. and White, J. L. *Polym. Eng. Sci.* 1975, **15,** 660
10 Katayama, K., Amano, T. and Nakamura, K. *Kolloid Z.Z. Polym.* 1968, **226,** 125
11 Dees, J. R. and Spruiell, J. E. *Appl. Polym. Sci.* 1974, **18,** 1055
12 Nadella, H., Henson, H. M., Spruiell, J. E. and White, J. L. *Appl. Polym. Sci.* 1977, **21,** 3013
13 Bankar, V., Spruiell J. E. and White, J. L. *Appl. Polym. Sci.* 1977, **21,** 2341
14 Hirami, M. and Tanimura, A. *Macromol. Sci. Phys., B1* 1985, **9,** 205
15 Chappel, F. P., Culpin, M. F., Gosden, R. G. and Trantere, T. C. *Appl. Chem.* 1964, **14,** 12
16 Ishizuka, O. and Koyama, K. *Polymer* 1977, **18,** 913
17 Haberkorn, H., Hahn, K., Breuer, H., Dorrer, H.-D. and Matthies, P. *J. Appl. Polym. Sci.* 1993, **47,** 1551
18 Elsner, G., Riekel, C. and Zachmann, H. G. *Adv. Polym. Sci.* 1985, **67,** 1
19 Gehrke, R., Riekel, C. and Zachmann, H. G. *Polymer* 1989, **30,** 1582
20 Cakmak, M., Teitge, A., Zachmann, H. G. and White, J. L. *J. Polym. Sci. Part. B: Polym. Phys.* 1993, **31,** 371
21 Zachmann, H. G., Bark, M., Röber, S., Teitge, A. and Cakmak, M., 29th Proc. Int. Man-Made Fibre Conf., Dornbirn, Austria, 1990
22 Hendrix, J. *IEEE Trans. Nucl. Sci., NS-31* 1984, **1,** 281
23 Hendrix, J. *Adv. Polym. Sci.* 1985, **67,** 59
24 Biangardi, H. J. and Zachmann, H. G. *Colloid Polym. Sci.* 1977, **62,** 71
25 Zachmann, H. G. and Günther, B. *Rheol. Acta* 1982, **21,** 427
26 Günter, B. and Zachmann, H. G. *Polymer* 1983, **24,** 1008
27 Katayama, K.-L. and Yoon, M.-G., Ref. 1, p. 207